

MultiFIT: A Multivariate Multiscale Framework for Independence Tests

Shai Gorsky

Department of Statistical Science, Duke University

and

Li Ma*

Department of Statistical Science, Duke University

December 14, 2024

Abstract

We present a framework for testing independence between two random vectors that is scalable to massive data. We break down the multivariate test into univariate tests of independence on a collection of 2×2 contingency tables, constructed by sequentially discretizing the sample space. This transforms a complex problem that traditionally requires quadratic computational complexity with respect to the sample size into one that scales almost linearly with the sample size. We further consider the scenario when the dimensionality of the random vectors grows large, in which case the curse of dimensionality arises in the proposed framework through an explosion in the number of univariate tests to be completed. To overcome this difficulty we propose a data-adaptive version of our method that completes a fraction of the univariate tests judged to be more likely to contain evidence for dependency. We demonstrate the tremendous computational advantage of the algorithm in comparison to existing approaches while achieving desirable statistical power through an extensive simulation study. In addition, we illustrate how our method can be used for learning the nature of the underlying dependency. We demonstrate the use of our method through analyzing a data set from flow cytometry.

Keywords: Nonparametric inference, multiple testing, unsupervised learning, scalable inference, massive data

*LM's research is partly supported by NSF grants DMS-1612889 and DMS-1749789.

1 Introduction

The problem of testing whether or not two random variables are independent appears frequently in the analysis of multivariate data. Our focus herein lies on the case when one or both variables are multivariate (i.e., random vectors), and in particular when the number of observations can potentially be massive (e.g., millions or even billions). This “big data” scenario presents a particular challenge to existing nonparametric independence tests, which typically require a computational complexity that scales at least quadratically with the sample size, making them impractical for massive data sets that are nowadays routinely generated in a variety of fields. In addition, we will allow the dimensionality of both random vectors to be moderately large, ranging up to about 100 dimensions each.

Testing independence and learning the dependency structure has been a fundamental statistical problem since the very beginning of modern statistics, and the last two decades have witnessed a surging of interest in this problem among statisticians, engineers and computer scientists. A variety of different methods have been proposed for testing independence between random vectors. For example, Székely and Rizzo [11] generalize the product-moment covariance and correlation to the distance covariance and correlation. This generalization has an equivalent definition in terms of empirical characteristic functions. Bakirov et al. [2], Fan et al. [3], and Meintanis and Iliopoulos [8] all developed nonparametric tests of independence based on the distance between the empirical joint characteristic function of the random vectors and the product of the marginal empirical characteristic functions of the two random vectors. Székely and Rizzo [12] further consider an asymptotic scenario with the dimensionality of the vectors increasing to infinity while keeping the sample size fixed. In a different vein, Heller et al. [5] form a test based on univariate tests of independence between the distances of each of the random vectors from a central point and perform inference based on permutations. In the machine learning literature, a class of kernel-based tests for independence have also become popular. For example, Gretton et al. [4] form a test based on the eigenspectrum of covariance operators in a reproducing kernel Hilbert spaces (RKHS). More recently, Pfister et al. [9] generalized this approach to the multivariate case by embedding the joint distribution into a RKHS. Most recently, Weihs et al. [14] defined a class of multivariate nonparametric measures which leads to

multivariate extensions of the Bergsma-Dassios sign covariance. Aside from these methods that are applicable to multivariate random vectors, there are also a number of methods proposed for testing independence of univariate random variables nonparametrically, some notable examples, among many others, include Reshef et al. [10], Wang et al. [13], and Zhang [15]. In particular, Ma and Mao [7] introduce a multiscale nonparametric test of univariate independence which we generalize and expand upon here.

The existing multivariate independence tests generally require the computation of statistics at a computational complexity that scales at least quadratically in the sample size, making them impractical for data sets with massive sample sizes. We will illustrate this computational bottleneck in our numerical studies. Aside from this fundamental difficulty, it is worth noting that, with a small number of notable exceptions (e.g., the “large p ” approximation in [12] and the Gamma approximation recently proposed in [9]), the existing multivariate methods also require resampling, in the form of either permutation or bootstrap, to complete inference such as evaluating the statistical significance. This additional computational burden makes practical applications of these methods very computationally expensive even for problems with moderate sample sizes.

Our approach aims at tackling the fundamental computational bottleneck in nonparametric multivariate independence testing without sacrificing the inferential validity in terms of accurate evaluation of the statistical significance. Our method adopts a general “divide-and-conquer” strategy commonly utilized in multi-scale inference. Specifically, instead of calculating a single test statistic for independence all at once, our method breaks apart the nonparametric multivariate test of independence into simple univariate independence tests on a collection of 2×2 contingency tables defined by sequentially discretizing the original sample space at a cascade of scales. This approach transforms a complex nonparametric testing problem into a multiple testing problem that can be addressed with a computational complexity that scales almost linearly with the sample size and completely avoids resampling. We establish a theoretical justification for this approach, showing that all types of dependency structures can be identified in this manner. We then further consider the scenario when the number of dimensions for the two vectors also grows large, in which case the curse of dimensionality arises in the proposed framework through an explosion in

the number of univariate tests to be completed. To overcome this difficulty, we propose a data-adaptive version of our method, which completes a fraction of the univariate tests judged to be more likely to contain evidence for dependency based on exploiting the spatial characteristics of the dependency structure in the data. We provide an inference recipe based on multiple testing adjustment that guarantees the validity in terms of controlling the family-wise error rate (FWER) for this adaptive algorithm. We carry out extensive numerical studies to illustrate both the computational efficiency and statistical performance of our proposed approach in comparison to the state-of-the-art.

2 Theoretical Framework

Without loss of generality, let $\Omega = [0, 1]^D$ be our sample space. Our formulation applies generally when some of the D dimensions of Ω are ordered categorical. Let $\mathbf{Z} = (Z_1, \dots, Z_D)$ be a random vector with a probability distribution F on the sample space Ω . **Figure 1** provides an illustration of the key concepts introduced in this section. First, we define a partition on each of the margins of Ω (for expositional simplicity, throughout the work we shall consider dyadic recursive partitioning on the margins of Ω as a sequence of nested partitions, although our framework applies generally to any sequence of nested partitions that generate the Borel σ -algebra):

Definition 2.1. *Level- k Marginal Dyadic Partition:*

\mathcal{P}^k is a *level- k marginal dyadic partition* if $\mathcal{P}^k = \left\{ \left[\frac{l-1}{2^k}, \frac{l}{2^k} \right) \right\}_{l \in \{1, \dots, 2^k\}}$.

A D -dimensional cuboid may be formed by taking the Cartesian product of one interval from each of the partitions, and we further consider the collection of all such cuboids with any $\mathbf{k} = (k_1, \dots, k_D) \in \mathbb{N}_0^D$ specifying the level of each dimension:

Definition 2.2. *\mathbf{k} -Cuboid:*

For any $\mathbf{k} = (k_1, \dots, k_D) \in \mathbb{N}_0^D$, we call a set $A \subset \Omega$ a *\mathbf{k} -cuboid* if it is of the form

$$A = A_1 \times A_2 \times \cdots \times A_D, \quad \text{with } A_d \in \mathcal{P}^{k_d} \text{ for all } d = 1, 2, \dots, D.$$

That is, a \mathbf{k} -cuboid is determined by some $\mathbf{l} = (l_1, \dots, l_D)$ with each $1 \leq l_d \leq 2^{k_d}$:

$$A = \prod_{d \in \{1, \dots, D\}} \left[\frac{l_d - 1}{2^{k_d}}, \frac{l_d}{2^{k_d}} \right).$$

Definition 2.3. \mathbf{k} -Stratum:

For any $\mathbf{k} = (k_1, \dots, k_D) \in \mathbb{N}_0^D$, we call the collection of all \mathbf{k} -cuboids the \mathbf{k} -stratum, which is

$$\mathcal{A}^{\mathbf{k}} = \mathcal{P}^{k_1} \times \dots \times \mathcal{P}^{k_D}.$$

Further, we call $|\mathbf{k}| = \sum_{d=1}^D k_d$ the *resolution* of the \mathbf{k} -stratum. We also say that a \mathbf{k} -cuboid is of resolution r when $|\mathbf{k}| = r$. Accordingly, if for $\mathbf{k}, \mathbf{k}' \in \mathbb{N}_0^D$, $|\mathbf{k}| = |\mathbf{k}'|$, then we say the \mathbf{k} -stratum is of the same resolution as \mathbf{k}' -stratum. Similarly, if $|\mathbf{k}| < |\mathbf{k}'|$, then the \mathbf{k} -stratum is of *lower* resolution than the \mathbf{k}' -stratum, or equivalently that latter is of *higher* resolution.

Also, we from now on denote $\mathbf{k}' \geq \mathbf{k}$ if $k'_1 \geq k_1, k'_2 \geq k_2, \dots, k'_D \geq k_D$. We denote $\mathbf{k}' > \mathbf{k}$ if $\mathbf{k}' \geq \mathbf{k}$ and there exists $d \in \{1, \dots, D\}$ such that $k'_d > k_d$.

If $\mathbf{k}' \geq \mathbf{k}$ we say that $\mathcal{A}^{\mathbf{k}'}$ is a *finer stratum* than $\mathcal{A}^{\mathbf{k}}$, which is said to be a *coarser stratum*. Note that if $\mathcal{A}^{\mathbf{k}'}$ is finer than $\mathcal{A}^{\mathbf{k}}$ then $|\mathbf{k}'|$ is higher than $|\mathbf{k}|$. However, the opposite does not necessarily hold.

Our goal is to test the independence of two random vectors. From now on then, let us consider testing the independence between the first D_x elements of \mathbf{Z} with the other $D_y = D - D_x$. That is, let $\mathbf{Z} = (\mathbf{X}, \mathbf{Y})$ where $\mathbf{X} \in [0, 1]^{D_x}$ and $\mathbf{Y} \in [0, 1]^{D_y}$. We next define a discretized form of independence which fully characterizes the multivariate independence in Theorem 2.1:

Definition 2.4. \mathbf{k} -independence:

For any $A \in \mathcal{A}^{\mathbf{k}}$, we can write $A = A_x \times A_y$ where

$$A_x = \bigtimes_{d=1}^{D_x} \left[\frac{l_d - 1}{2^{k_d}}, \frac{l_d}{2^{k_d}} \right) \text{ and } A_y = \bigtimes_{d=D_x+1}^D \left[\frac{l_d - 1}{2^{k_d}}, \frac{l_d}{2^{k_d}} \right).$$

We say that \mathbf{X} and \mathbf{Y} are \mathbf{k} -independent and write it as $\mathbf{X} \perp_{\mathbf{k}} \mathbf{Y}$ if for any $A \in \mathcal{A}^{\mathbf{k}}$,

$$\mathbb{P}(\mathbf{X} \in A_x, \mathbf{Y} \in A_y) = \mathbb{P}(\mathbf{X} \in A_x) \cdot \mathbb{P}(\mathbf{Y} \in A_y).$$

Theorem 2.1.

$$\mathbf{X} \perp \mathbf{Y} \Leftrightarrow \mathbf{X} \perp_{\mathbf{k}} \mathbf{Y} \text{ for all } \mathbf{k} \in \mathbb{N}_0^D.$$

We next define a collection of log odd ratios (LORs), each corresponding to the division of one of the $D_x \times D_y$ faces of a \mathbf{k} -cuboid A into four quadrants. In Theorem 2.2 we show how these LORs characterize \mathbf{k} -dependency.

Definition 2.5. (i, j) -quadrants of a \mathbf{k} -cuboid:

For every \mathbf{k} -cuboid $A \in \mathcal{A}^{\mathbf{k}}$ and $i, j \in \{1, \dots, D\}$, one can partition A into four blocks by dividing A in the (i, j) th face (that is, the side of A spanned by the i th and j th dimensions) into four quadrants while keeping the other dimensions intact.

$$A = A_{ij}^{00} \sqcup A_{ij}^{01} \sqcup A_{ij}^{10} \sqcup A_{ij}^{11},$$

where for $a, b \in \{0, 1\}$,

$$A_{ij}^{ab} = \bigtimes_{d=1}^D \begin{cases} \left[\frac{2l_d-2+a}{2^{k_d+1}}, \frac{2l_d-1+a}{2^{k_d+1}} \right) & \text{if } d = i \\ \left[\frac{2l_d-2+b}{2^{k_d+1}}, \frac{2l_d-1+b}{2^{k_d+1}} \right) & \text{if } d = j \\ \left[\frac{l_d-1}{2^{k_d}}, \frac{l_d}{2^{k_d}} \right) & \text{if } d \in \{1, \dots, D\} \setminus \{i, j\} \end{cases}.$$

Definition 2.6. (i, j) -face log odds ratio of a \mathbf{k} -cuboid:

For any \mathbf{k} -cuboid $A \in \mathcal{A}^{\mathbf{k}}$, $1 \leq i \leq D_x$, and $D_x < j \leq D$, we call $\theta_{ij}(A) = \log \frac{F(A_{ij}^{00}) \cdot F(A_{ij}^{11})}{F(A_{ij}^{01}) \cdot F(A_{ij}^{10})}$ the (i, j) -face log odds ratio (LOR) of the \mathbf{k} -cuboid A .

The following lemma shows that if \mathbf{X} and \mathbf{Y} are \mathbf{k} -independent, i.e. as two discrete random variables supported on a \mathbf{k} -stratum, they are also independent on all coarser strata. This will enable our coarse-to-fine scanning test strategy we present in Section 2.1.

Lemma 2.1. *If $\mathbf{X} \perp_{\mathbf{k}} \mathbf{Y}$ then $\mathbf{X} \perp_{\mathbf{k}'} \mathbf{Y}$ for all $\mathbf{k}' \leq \mathbf{k}$.*

Definition 2.7. (i, j) -face coarser strata:

Given $\mathbf{k} \in \mathbb{N}_0^D$ and $i, j \in \{1, \dots, D\}$ denote

$$[k_i, k_j] = \{ \mathbf{k}' \in \mathbb{N}_0^D : k'_i < k_i, k'_j < k_j \text{ and } k'_d = k_d \text{ for all } d \in \{1, \dots, D\} \setminus \{i, j\} \}$$

and let then

$$\mathcal{A}^{[k_i, k_j]} = \bigcup_{\mathbf{k}' \in [k_i, k_j]} \mathcal{A}^{\mathbf{k}'}$$

be the union of all strata that are coarser than the stratum $\mathcal{A}^{\mathbf{k}}$ on the (i, j) -face of A .

Our next theorem ties the \mathbf{k} -independence of the random vectors \mathbf{X} and \mathbf{Y} with the (i, j) -face LORs:

Theorem 2.2. *For any $\mathbf{k} > \mathbf{0}_D$*

$$\mathbf{X} \perp_{\mathbf{k}} \mathbf{Y} \Leftrightarrow \theta_{ij}(A) = 0$$

$$\forall i \in \{1, 2, \dots, D_x\}, j \in \{D_x + 1, \dots, D\}, A \in \mathcal{A}^{[k_i, k_j]}.$$

We are now ready to articulate the main problem at hand: testing the null hypothesis $H_0 : \mathbf{X} \perp \mathbf{Y}$ vs. the alternative $H_1 : \textit{else}$.

Our aim is to utilize tests on the LORs for the 2×2 tables that discretize the data at different resolutions. For this aim we first define the counts of data points in each cuboid:

Definition 2.8. *Cuboid Counts:*

Suppose $\mathbf{Z}_1, \dots, \mathbf{Z}_n$ are i.i.d draws from F . Then for any $A \in \mathcal{A}^{\mathbf{k}}$, let $n(A)$ be the number of observations in A . That is, $n(A) = |\{c : \mathbf{Z}_c \in A\}|$.

Lastly, the following defines the 2×2 contingency tables to which we will apply standard univariate tests of independence in order to test for $\theta_{ij}(A) = 0$:

Definition 2.9. *(i, j) -table of a \mathbf{k} -cuboid:*

With an i.i.d. sample from F , for any $A \in \mathcal{A}^{\mathbf{k}}$ and $i, j \in \{1, \dots, D\}$, we call the 2×2 contingency table given by

$$\mathbf{n}_{ij}(A) = \{n(A_{ij}^{00}), n(A_{ij}^{01}), n(A_{ij}^{10}), n(A_{ij}^{11})\} \quad \text{or} \quad \begin{array}{|c|c|} \hline n(A_{ij}^{00}) & n(A_{ij}^{01}) \\ \hline n(A_{ij}^{10}) & n(A_{ij}^{11}) \\ \hline \end{array}$$

the (i, j) -table of A .

See **Figure 1** for an illustration of the above definitions. Combining all of the above definitions with Theorem 2.1, Lemma 2.1 and Theorem 2.2 we get the main thrust of the coarse-to-fine strategy in our framework: start by testing for the null that all of the (i, j) -face LORs are 0 for the cuboid at resolution 0 (the entire sample space), and continue to test cuboids in higher and higher resolutions. In theory, one needs infinitely many observations in order to test the right hand side of Theorem 2.2. With finite samples, one should only test the hypotheses on cuboids up to some maximal resolution r as cuboids at higher resolutions

will eventually be containing too few, if any, observations to allow reliable inference on the corresponding LORs. In practice, one can let the maximal resolution grow logarithmically with the sample size.

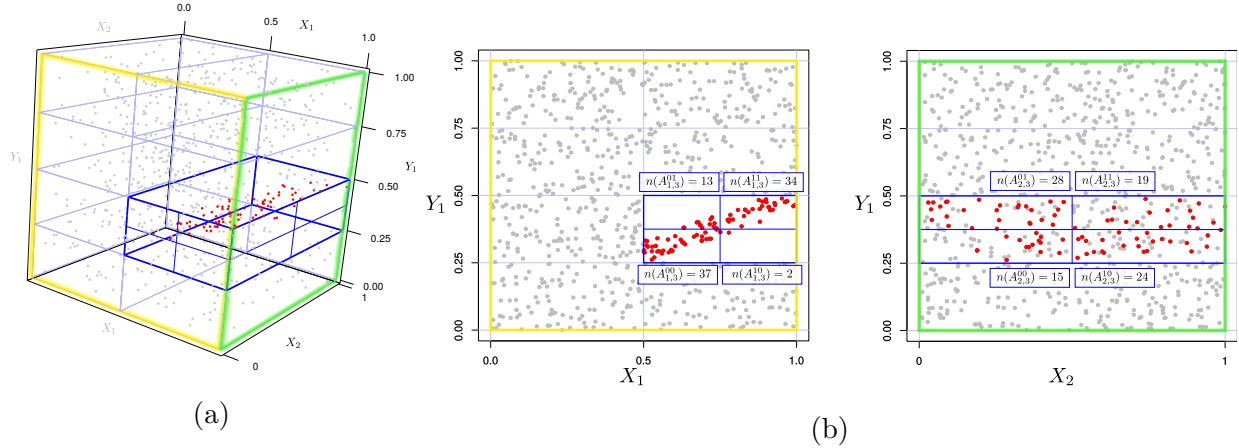


Figure 1: Illustration of the key concepts.

(a) A 3D view of a \mathbf{k} -cuboid and a \mathbf{k} -stratum where $\mathbf{X} = (X_1, X_2) = (Z_1, Z_2)$ and $\mathbf{Y} = Y_1 = Z_3$ (i.e. $D_x = 2$ and $D_y = 1$). The thin blue lines delineate all \mathbf{k} -cuboids with $\mathbf{k} = (1, 0, 2)$. The thick blue lines delineate the cuboid A for which $\mathbf{l} = (2, 1, 2)$, i.e., $A = ([0.5, 1) \times [0, 1)) \times [0.25, 0.5)$. The grey points are all data points outside of A , the red points are inside A .

(b) 2D views of the $(1, 3)$ -face and the $(2, 3)$ -face of A . Left: Testing the null $\theta_{1,3}(A) = 0$, using the 2×2 table $\mathbf{n}_{1,3}(A) = (37, 13, 2, 34)$. Right: testing the null $\theta_{2,3}(A) = 0$ using the 2×2 table $\mathbf{n}_{2,3}(A) = (15, 28, 24, 19)$.

2.1 The Data-Adaptive MultiFIT Algorithm

Our algorithm is based on a coarse-to-fine multiple testing strategy. Prior to providing our algorithm we highlight a fundamental difficulty: the huge number of tests required for an exhaustive coarse-to-fine test when the dimensionality of the random vectors grows. Suppose the dimensionality of \mathbf{X} is D_x , the dimensionality of \mathbf{Y} is D_y , $D = D_x + D_y$ and let $r = |\mathbf{k}|$. In a given \mathbf{k} -stratum there are 2^r \mathbf{k} -cuboids. Further, in a resolution r there are $\binom{r+D-1}{D-1}$ strata (the number of non-commutative ways to form the sum r from D

non-negative integers). For each cuboid we need to test the LOR on $D_x \times D_y$ (i, j) -faces. Thus, in order to exhaustively test all cuboids up to resolution r we need to perform $\sum_{\rho=0}^r D_x \cdot D_y \cdot 2^\rho \cdot \binom{\rho+D-1}{D-1}$ tests. For example, with $D_x = 40$, $D_y = 40$, we would have to perform $1.85 \cdot 10^{38}$ tests up to a maximum resolution of 4. One may alleviate the problem by carrying out tests on tables whose column and row marginal totals exceed a threshold, for otherwise the table cannot have generated a statistically significant result anyway. Such a sample size screening is always recommended. However, with a substantial sample size, this alone will not suffice to reduce the number of tests to a tractable one when the number of dimensions is large. Beyond the consideration of computational practicality, reducing the number of tests is also desirable for the sake of statistical performance. Specifically, for every additional test we carry out there is a price to pay in multiple testing control, and thus it is important to be discreet in choosing the tests to complete.

We propose a data-adaptive strategy for handling this difficulty by completing the tests on tables that are “descendants” of the tables in coarser strata that have generated the most significant p -values. This strategy is motivated by the spatial characteristics of dependency structures—when \mathbf{X} and \mathbf{Y} are dependent, then nearby and nested cuboids tend to contain empirical evidence for the dependency in a correlated manner. Thus using the statistical evidence at coarser strata to inform the portion of tables to scan in higher resolutions can lead to effective detection of the dependency structure.

We now are ready to present the full data-adaptive **MultiFIT** algorithm:

- (0) Take the entire sample space, a $\mathbf{0}$ -cuboid, as the *parent* cuboid of resolution $r = 0$.
- (1) Apply a univariate test of independence to the $D_x \cdot D_y$ (i, j) -tables of each parent cuboid.
- (2) Select the (i, j) -faces producing the top M most extreme p -values from the above tests.
- (3) For every (i, j) -face selected above divide the parent cuboid A into four *child* cuboids of resolution $r + 1$: halve the parent cuboid along the i th and the j th margins respectively, each generating two children.
- (4) On each of the $M \cdot 4 \cdot D_x \cdot D_y$ child cuboids, repeat Steps (1) through (4) until either

the number of observations in a cuboid falls below a preset threshold or a maximal resolution is achieved.

Once the algorithm terminates on the above steps, we have computed all the p -values. We then control for multiple testing using one of the following methods:

- (5) Execute Holm’s step-down procedure [6], or a modified Holm method, developed by Zhu and Guo [16]. Both strongly control the FWER under arbitrary dependence structures of the p -values.

The univariate tests of independence for 2×2 tables for step (1) our implementation offers are: two-sided Fisher’s exact test, a two-tailed approximate z -test for the hypergeometric distribution, the likelihood-ratio test of independence and the χ^2 -test. We emphasize that our framework is agnostic to the specific test of independence that is used in this step: the researcher may apply tests with different advantages, according to needs.

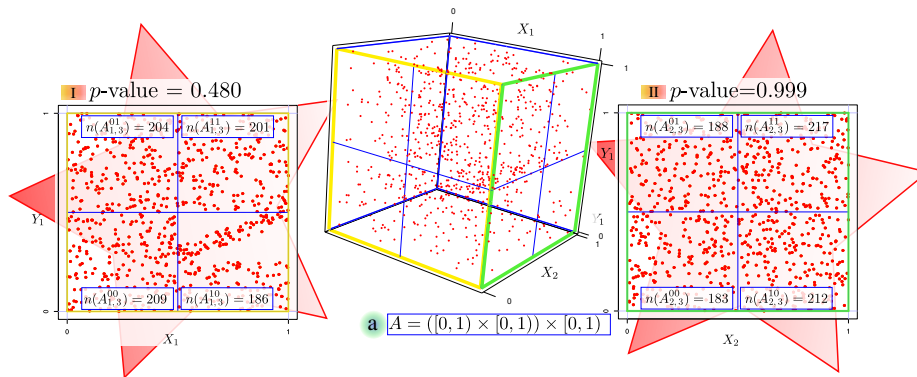


Figure 2: Illustration of the algorithm, resolution 0 cuboids and tests.

Step (0): the cuboid (a) is the entire space A .

Step (1): cuboid’s (a) two ($= D_x \cdot D_y$) (i, j)-faces, corresponding tables and p -values are shown in (I) and (II).

Step (2): As we have two p -values in resolution 0 and choose at each resolution the 3 tests with the most extreme p -values, we select here both faces (stars denote selected faces).

Figure 2 and **Figure 3** illustrate an application steps (0) to (4) of the algorithm in three dimensions. At each resolution we choose the 3 tables with the most extreme p -values resulting from Fisher’s exact tests. Here, $D_x = 2$ with $(X_1, X_2) = (Z_1, Z_2)$ and $D_y = 1$ with

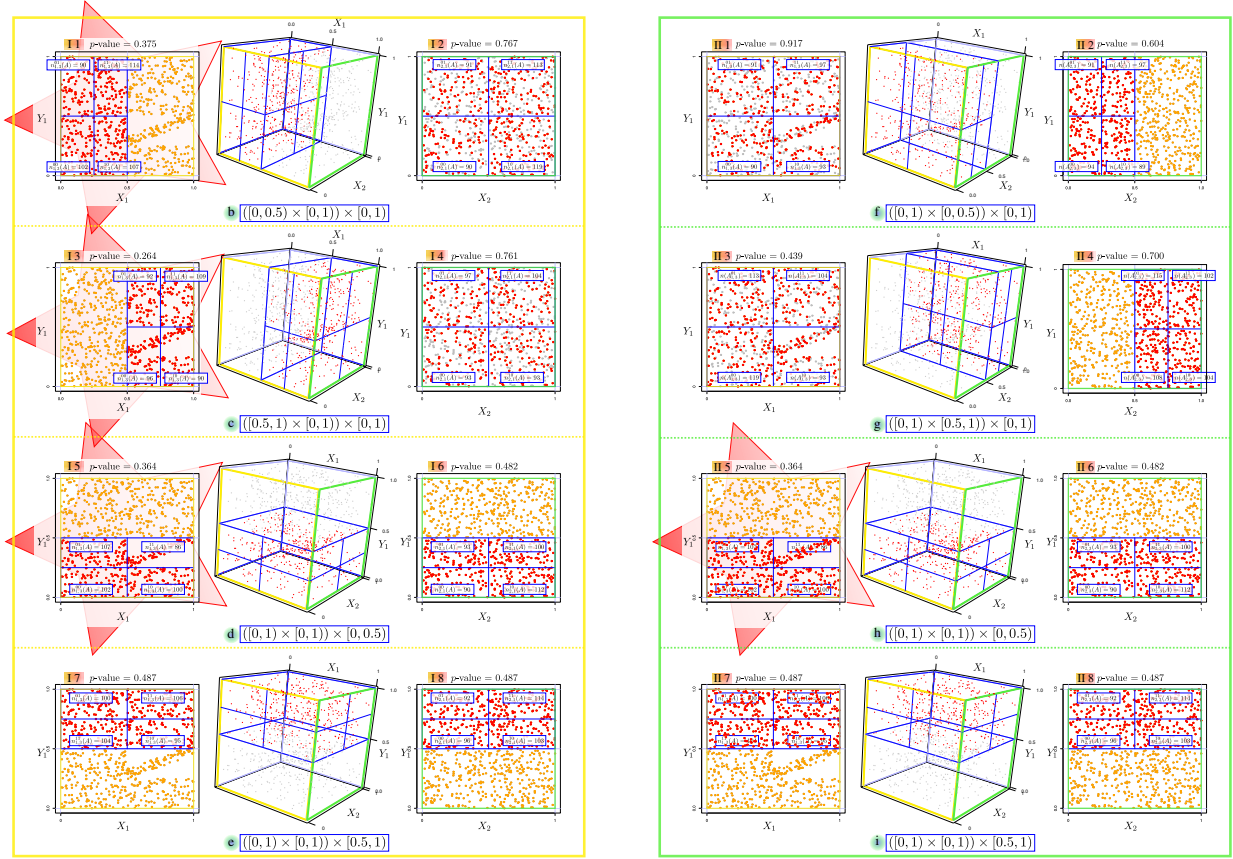


Figure 3: Illustration of the algorithm, resolution 1 cuboids and tests.

Resolution 0, Step (3): The resolution 1 cuboids (b)-(e) result from the selection of the (1, 3)-face (I) in resolution 0: the parent cuboid is (a) (see **Figure 2**). It is split at $X_1 = 0.5$ to the child cuboids (b) and (c) and at $Z_3 = Y_1 = 0.5$ to the child cuboids (d) and (e). The resolution 1 cuboids (f)-(i) result from the selection of the (2, 3)-face (II): the corresponding parent is again the cuboid (a). It is split at $X_2 = 0.5$ to the child cuboids (f) and (g) and at $Z_3 = Y_1 = 0.5$ to the child cuboids (h) and (i).

Resolution 1, steps (1)-(2): we then choose the 3 tables with the most extreme p -values out of the resolution 1 tests I.1-I.8 and II.1-II.8. Note: cuboids (d) and (h) are the same, as well as cuboids (e) and (i). Hence, although four faces are marked as selected, we indeed choose three.

$Y_1 = Z_3$. Observations in grey are outside a cuboid and observations in red are in a cuboid. Observations in orange are outside a cuboid, and were to be included in it if the shown face were not halved.

3 Numerical Examples

3.1 Computational Scalability

We compare the performance of our method with the Heller-Heller-Gorfine (HHG) multivariate test of association [5], the Distance Covariance (DCov) method of [11] and the kernel based method (dHSIC) of [9]. They are powerful as the main competitors and are the fastest multivariate tests of independence we are aware of. `MultiFIT` presents excellent scalability in sample size: approximately $\mathcal{O}(n \log n)$ (including multiple testing adjustment). HHG, DCov and dHSIC without the Gamma approximation scale approximately $\mathcal{O}(n^2)$ in the number of observations. The Gamma approximation method of dHSIC is faster, yet still outperformed by `MultiFIT` for larger sample sizes. It is also worth noting that with the Gamma approximation dHSIC loses its theoretical guarantee on inference validity, which our approach maintains. **Figure 4** presents some results that demonstrate the scaling properties of our algorithm compared to that of the HHG, DCov and dHSIC methods as the number of observations and the dimensionality grow. All were run on the same computer until the memory requirements of each of the methods surpassed those available to it. For `MultiFIT` we present the duration of execution for (i) Fisher’s exact test with the modified Holm correction - the most computationally intense testing and adjustment methods, and (ii) one with the lightest computation: the normally approximated hypergeometric test with Holm’s correction, both when choosing the top-4 ($M = 4$) or top-100 ($M = 100$) ranking tests at each resolution.

3.2 Power

We test the competing algorithms for $\mathbf{X} = (X_1, X_2)$ and $\mathbf{Y} = (Y_1, Y_2)$ where X_1 and Y_1 are independently normally distributed, and X_2 and Y_2 are dependent according to different scenarios, as illustrated in **Figure 5** and detailed in **Table 1**. We performed

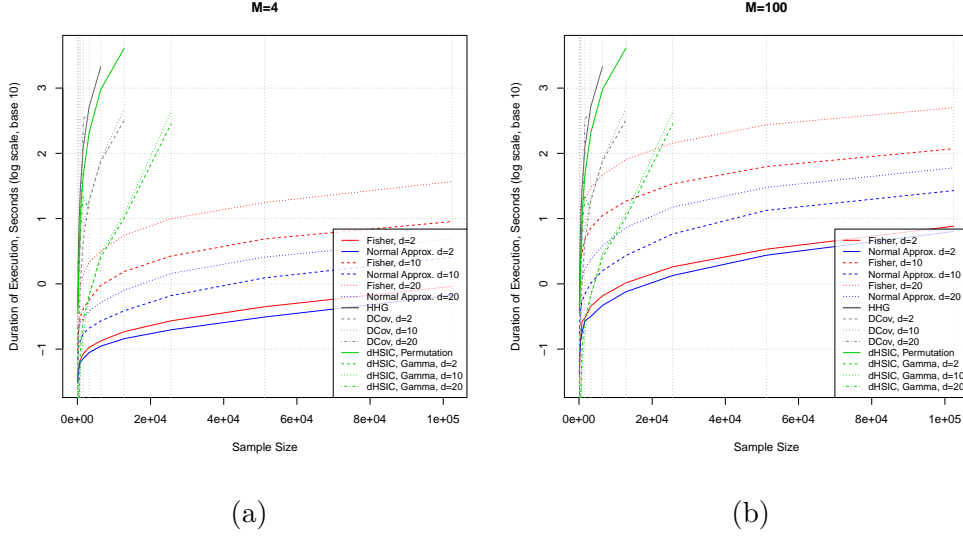


Figure 4: Scaling: a comparison of MultiFIT, HHG, DCov and dHSIC.

In both panels, $D_x = D_y = d$ for all methods. MultiFIT selects in (a) the top 4 ranking tests in each resolution, and in (b) the top 100 ranking tests in each resolution.

2000 simulations for each scenario and noise level, all with a significance level of 0.05. MultiFIT scales the data with a marginal rank transformation by default, thereby bisecting the margins at resolution 0 along their medians. The HHG, DCov and dHSIC algorithms performed very poorly on the original data. In order to provide a fair comparison, we also applied them to the rank transformed data.

In the execution of MultiFIT we test the 100 top ranking tests for each resolution with Fisher’s exact test and mid- p corrected p -values (see [1] for a discussion on the mid- p correction). Notice that in the “circle”, “checkerboard” and “local” scenarios the cell counts at resolution 0 will be roughly equal. Were the algorithm to stop testing at resolution 0, no dependency were likely to be detected. However, as the test will continue to test higher resolutions it may indeed detect the dependencies as they are reflected in the 2×2 tables. For the “circle” and “checkerboard” scenarios we make no adjustments in the tuning parameters. For the “local” scenario, where a signal is embedded in a small sub-portion of the margins X_2 and Y_2 and all other regions are independent, we applied the algorithm in such a way as to guarantee an exhaustive coverage up to and including resolution 4, and from there on continue testing the top 100 ranked tests for each of the higher resolutions.

Table 1: Simulation Scenarios

Scenario	# of Data Points	Maximal Resolution	Simulation Setting
Sin	300	4	$X_1 = Z, Y_1 = Z', X_2 = U,$ $Y_2 = \sin(5\pi \cdot X_2) + 4\epsilon$
Circular	300	4	$X_1 = Z, Y_1 = Z',$ $X_2 = \cos(\theta) + \epsilon, Y_2 = \sin(\theta) + \epsilon'$
Checkerboard	500	5	$X_1 = Z, Y_1 = Z', X_2 = W + \epsilon,$ $Y_2 = \begin{cases} V_1 + \epsilon', & \text{if } W \text{ is odd} \\ V_2 + \epsilon', & \text{if } W \text{ is even} \end{cases}$
Linear	300	4	$X_1 = Z, Y_1 = Z', X_2 = U,$ $Y_2 = X_2 + 3\epsilon$
Parabolic	300	4	$X_1 = Z, Y_1 = Z', X_2 = U,$ $Y_2 = (X_2 - 0.5)^2 + 0.75\epsilon$
Local	1000	6	$X_1 = Z, Y_1 = Z', X_2 = Z'',$ $Y_2 = \begin{cases} X_2 + 1/6 \cdot \epsilon & \text{if } 0 < X_2, Z''' < 0.7 \\ Z''', & \text{otherwise} \end{cases}$

Six simulation scenarios. In all cases, Z, Z' are i.i.d $N(0, 1)$. At each noise level $l = 1, 2, \dots, 20$, ϵ, ϵ' and ϵ'' are i.i.d $N(0, (l/20)^2)$, and the following random variables are all independent: $U \sim \text{Uniform}(0, 1)$, $\theta \sim \text{Uniform}(-\pi, \pi)$, $W \sim \text{Multi-Bern}(\{1, 2, 3, 4, 5\}, (1/5, 1/5, 1/5, 1/5, 1/5))$, $V_1 \sim \text{Multi-Bern}(\{1, 3, 5\}, (1/3, 1/3, 1/3))$, $V_2 \sim \text{Multi-Bern}(\{2, 4\}, (1/2, 1/2))$ and Z'', Z''' are i.i.d $N(0, 1)$. The maximal resolution is the algorithm's default: $\lceil \log_2(n/10) \rceil$ where n is the number of data points. In all cases we apply the screening rule that only tests pairs of margins if the grand total is at least 25, and all four marginal totals are at least 10.

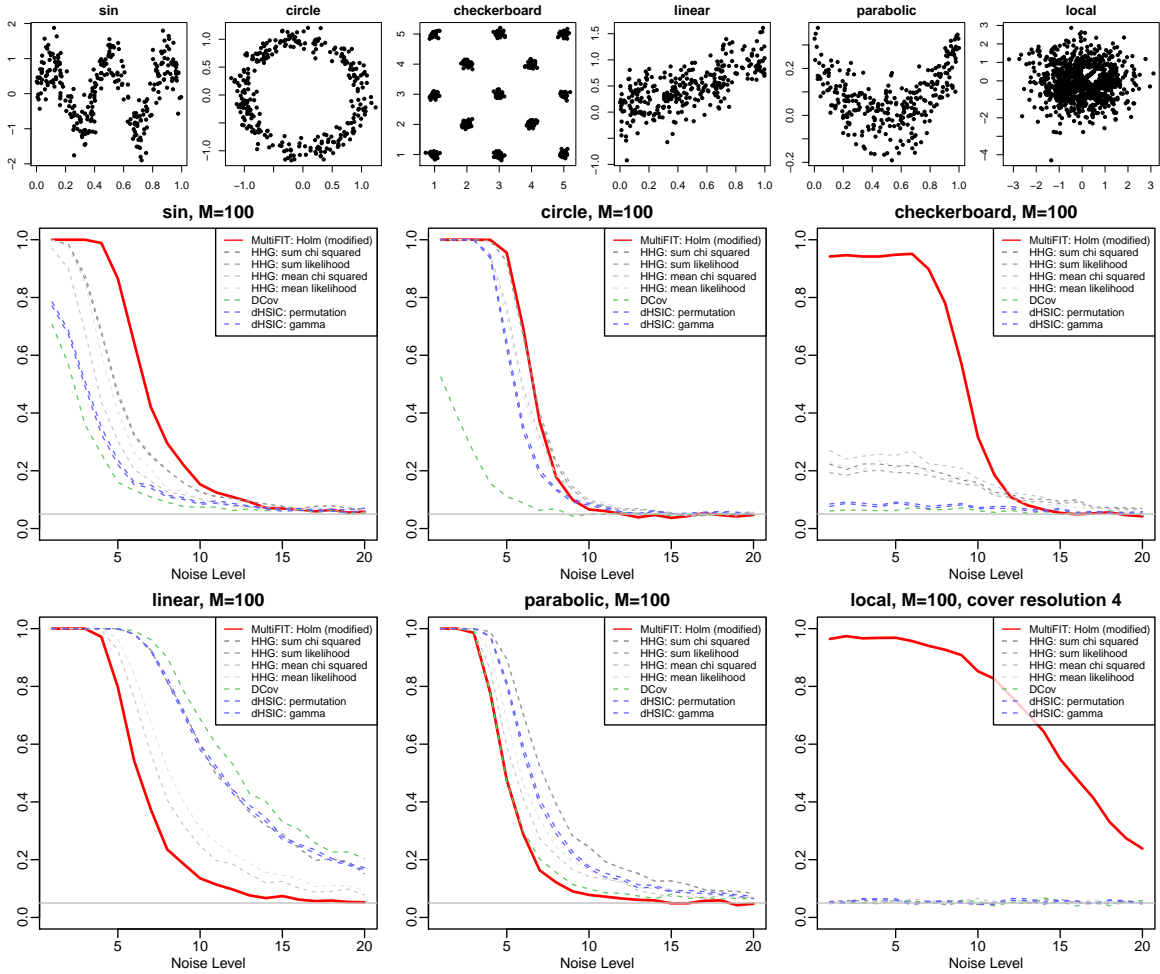


Figure 5: A comparison of simulated power.

Top row: dependent margins of scenarios with noise level 2.

Bottom rows: estimated power

Our algorithm outperforms the HHG, DCov and dHSIC algorithms for the “sin”, “circle”, “checkerboard” and “local” scenarios, the cases that are richer with local structures. The picture is different in the “linear” and “parabolic” scenarios: they are “more global”, and there HHG and dHSIC outperform our algorithm (where DCov does so only in the “linear” case). This is explained by the fact that the signal is observable almost entirely in the coarsest level, and as we go into higher resolutions we merely add insignificant tests that reduce the overall power. When we test these “more global” scenarios with a maximal resolution lower than the default of $\lfloor \log_2(n/10) \rfloor$, MultiFIT achieves more power.

3.3 Additional Examples

In this section we provide two examples that highlight `MultiFIT`'s unique ability of learning the dependency structure in the data. The examples in the previous sections focused on demonstrating our algorithm on signals that are mainly marginal. Here, we broaden the canvas.

Example 3.3.1. *A Rotated Circle:*

In this scenario, we take \mathbf{X} and \mathbf{Y} to be each of three dimensions, with 800 data points. We first generate a ‘circle’ scenario so that X_1 , Y_1 , X_2 , and Y_2 are all i.i.d. standard normals. Take $X_3 = \cos(\theta) + \epsilon$, $Y_3 = \sin(\theta) + \epsilon'$ where ϵ and ϵ' are i.i.d $N(0, (1/10)^2)$ and $\theta \sim \text{Uniform}(-\pi, \pi)$. We then rotate the circle by $\pi/4$ degrees in the X_2 - X_3 - Y_3 space by applying:

$$\begin{bmatrix} \cos(\pi/4) & -\sin(\pi/4) & 0 \\ \sin(\pi/4) & \cos(\pi/4) & 0 \\ 0 & 0 & 1 \end{bmatrix} \begin{bmatrix} | & | & | \\ X_2 & X_3 & Y_3 \\ | & | & | \end{bmatrix}$$

The rotated circle is harder to see by examining the margins. See **Figure 6** for the marginal views of the original and the rotated setting. **Figure 7** shows the tests our algorithm identified with p -values below 0.0002.

Example 3.3.2. *Superimposed Sine Waves:*

In this scenario, we follow the suggestion by Reshef et al. [10] and examine our algorithm’s ability to (i) detect a signal that is made of two sine waves in different frequencies, and (ii) given a third dimension that determines which data points belong to which wave, to see if our algorithm successfully identifies this relation.

We take \mathbf{X} to be a two dimensional random variable and \mathbf{Y} to be one dimensional, all with 550 data points. Define $X_1 \sim U(0, 1)$, $X_2 \sim \text{Beta}(0.3, 0.3)$ independent of X_1 , and define:

$$Y = \begin{cases} \sin(10 \cdot X_1) + \epsilon, & \text{if } X_2 > 0.75 \\ \sin(40 \cdot X_1) + \epsilon, & \text{if } X_2 \leq 0.75 \end{cases}$$

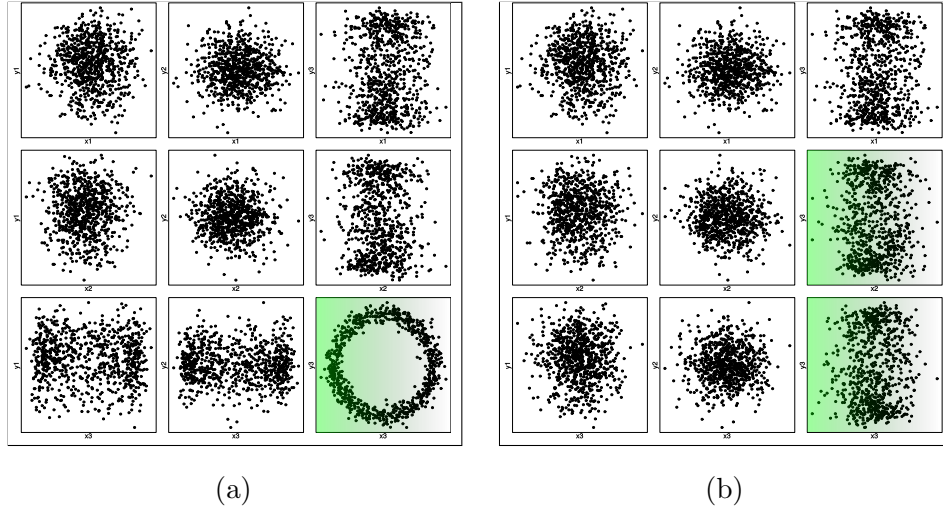


Figure 6: Marginal views of a circle and a rotated circle in a 3×3 setting. The signal in the original setting (a) is easily visible in the marginal view. Once rotated, the signal is spread between more margins, and harder to detect with the naked eye (b).

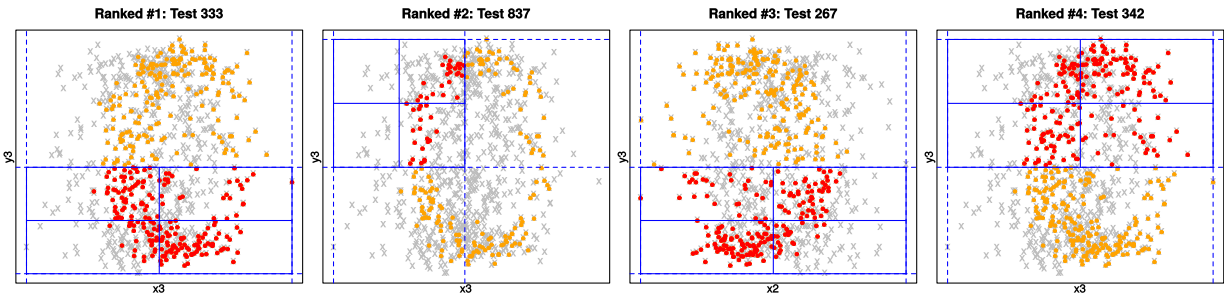


Figure 7: Tests for the rotated circle with p -values below 0.0002. The testing was performed with Fisher's exact test on each 2×2 table when the children of the top-4 ranking tests were considered in each resolution. The tests ranking #1, #2 and #4 are in the X_3 - Y_3 plane, and are conditioned on X_2 , and the third ranking test is in the X_2 - Y_3 plane (see supplementary material for more details)

See **Figure 8** for the marginal views of the superimposed setting. **Figure 9** shows the tests our algorithm identified which separate the sine waves (see supplementary material for more details).

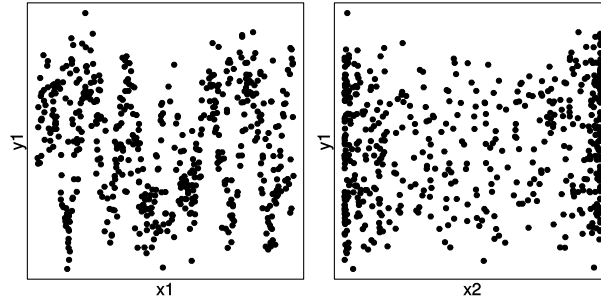


Figure 8: Marginal views of the superimposed sine setting. The X_1 - Y_1 margin (left) shows the superimposed sine waves.

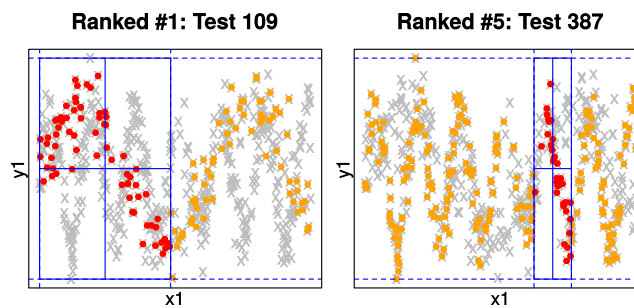


Figure 9: Tests for the superimposed sine setting with p -values below 0.05. The testing was performed with Fisher’s exact test when the children of the top 100 ranking tests were considered in each resolution, and the p -values resented here are the Modified-Holm adjusted p -values. The first and third ranking tests identify the separate signals in the X_1 - Y plane, as determined by X_2 .

4 Application to Real Data

Flow cytometer is the standard biological assay used to measure single cell features known as markers, and is commonly used to quantify the relative frequencies of cell subsets in blood or disaggregated tissue. These features may be general physical, chemical or biological properties of a cell.

For the evaluation, we used flow cytometry samples generated by an antibody panel designed to identify activated T cell subsets. We show the results of the dependency analysis on a single illustrative sample with 353,586 cells. For the analysis, we separated the markers into a vector of four “basic” markers (dump, CD3, CD4, CD8) and a vector of four

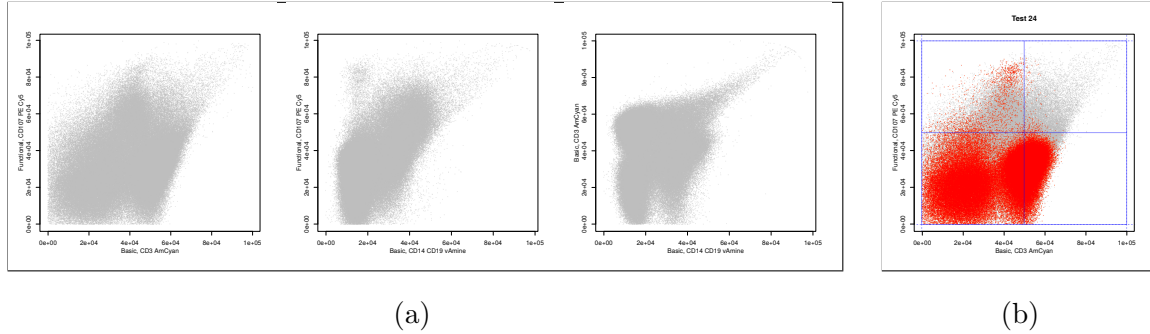


Figure 10: Flow cytometry analysis.

- (a) Three marginal views of biomarker data.
- (b) A Significant Test which was identified by **MultiFIT**.

“functional” markers (IFN, TNF, IL-2 and CD107). The basic markers are used in practice to first identify viable T cells by exclusion using the “dump” and CD3 markers, and then to further partition T cells into CD4-positive (“helper”) and CD8-positive (“cytotoxic”) subsets. The functional markers are used to identify the activation status of these T cell subsets and their functional effector capabilities (IL-2 is a T cell growth factor, IFN and TNF are inflammatory cytokines, and CD107 is a component of the mechanism used by T cells to directly kill infected and cancer cells).

The three plots of **Figure 10a** show several marginal relations between biomarkers in our sample. It is not a-priori clear where interesting relations between them may lay.

We applied the **MultiFIT** algorithm using the normal approximation testing method with Holm’s multiple testing adjustment. At each resolution we chose to further test the children of the top 10 ranking tests. The execution time of the algorithm in this setting is approximately 5 seconds on a laptop computer utilizing a single 3.00GHz Intel[®] Xeon(R) E3-1505M v6 CPU core. As the sample size is very large and the data clearly have strong marginal dependencies, **MultiFIT** identified many significant tests. None of **HHG**, **DCov** and **dHSIC** was able to handle this amount of data and all ended in runtime or overflow errors. See also **Figure 4** for an illustration of the limits on the amount of data each of the methods can handle in lower dimensions.

The algorithm not only picks up strong marginal signals, but is also capable of identifying interesting joint structures. The plot in **Figure 10b** shows the same margins as the leftmost

plot. Added to it are red points, the observations who were tested in Test 24 that was performed, and blue lines that delineate the quadrants along which the discretization was performed. The tested margins are the functional marker CD107 vs. the basic marker CD3, both are conditioned on the basic “dump” marker having values between 0.66 and 14375.84. The resulting p -value for this test is $0.6 \cdot 10^{-305}$ - machine zero. Indeed, when examining the points that are actually tested here, an interesting pattern emerges, one which divides the main cluster of points into three sub-clusters. Thus, a non-trivial joint dependence structure between three markers is revealed from the many possible subsets of margins as a byproduct of our algorithm. See the supplemental material for additional information on why Test 24 was chosen out of the many tests that were identified with p -value of machine zero.

5 Conclusion

We have presented a scalable framework for nonparametrically testing the independence of random vectors that achieve high computational scalability and statistical power. It is applicable to continuous, discrete and mixed random variables, excels in identifying non-linear and localized patterns of dependency, provides insights as to the structure of detected dependencies, and scales almost linearly in the number of observations. Our simulation studies have demonstrated that the estimated power of our algorithm compares favorably to that of the main competitors on many scenarios, rendering our method a strong candidate for a wide variety of real life applications. We have implemented an R package and made it freely available at <https://cran.r-project.org/web/packages/MultiFit/index.html>.

6 Acknowledgements

We thank Dr. Cliburn Chan for providing the flow cytometry data and for fruitful discussions about its potential analyses. The data is collected through an EQAPOL collaboration with federal funds from the National Institute of Allergy and Infectious Diseases, National Institutes of Health, Contract Number HHSN272201700061C.

References

- [1] A. Agresti and A. Gottard. Nonconservative exact small-sample inference for discrete data. *Computational Statistics & Data Analysis*, 51(12):6447 – 6458, 2007.
- [2] N. K. Bakirov, M. L. Rizzo, and G. J. Székely. A multivariate nonparametric test of independence. *Journal of Multivariate Analysis*, 97:1742–1756, 2006.
- [3] Y. Fan, P. L. de Micheaux, S. Penev, and D. Salopek. Multivariate nonparametric test of independence. *Journal of Multivariate Analysis*, 153:189–210, 2017.
- [4] A. Gretton, K. Fukumizu, C. H. Teo, L. Song, B. Schölkopf, and A. J. Smola. A kernel statistical test of independence. In J. C. Platt, D. Koller, Y. Singer, and S. T. Roweis, editors, *Advances in Neural Information Processing Systems 20*, pages 585–592. Curran Associates, Inc., 2008.
- [5] R. Heller, Y. Heller, and M. Gorfine. A consistent multivariate test of association based on ranks of distances. *Biometrika*, 100:503–510, 2013.
- [6] S. Holm. A simple sequentially rejective multiple test procedure. *Scandinavian Journal of Statistics*, 6(2):65–70, 1979.
- [7] L. Ma and J. Mao. Fisher exact scanning for dependency. *Journal of the American Statistical Association*, 2018. Accepted.
- [8] S. G. Meintanis and G. Iliopoulos. Fourier methods for testing multivariate independence. *Computational Statistics & Data Analysis*, 52:1884–1895, 2008.
- [9] N. Pfister, P. Bühlmann, B. Schölkopf, and J. Peters. Kernel-based tests for joint independence. *Journal of the Royal Statistical Society: Series B (Statistical Methodology)*, 80(1):5–31, 2018.
- [10] D. N. Reshef, Y. A. Reshef, H. K. Finucane, S. R. Grossman, G. McVean, P. J. Turnbaugh, E. S. Lander, M. Mitzenmacher, and P. C. Sabeti. Detecting novel associations in large data sets. *Science*, 334(6062):1518–1524, 2011.

- [11] G. J. Székely and M. L. Rizzo. Brownian distance covariance. *The Annals of Applied Statistics*, 3(4):1236–1265, 2009.
- [12] G. J. Székely and M. L. Rizzo. The distance correlation t-test of independence in high dimension. *Journal of Multivariate Analysis*, 117:193 – 213, 2013.
- [13] X. Wang, B. Jiang, and J. S. Liu. Generalized R-squared for detecting dependence. preprint, November 2016.
- [14] L. Weihs, M. Drton, and N. Meinshausen. Symmetric rank covariances: a generalized framework for nonparametric measures of dependence. *Biometrika*, 105(3):547–562, 2018.
- [15] K. Zhang. BET on independence. preprint, November 2017.
- [16] Y. Zhu and W. Guo. Familywise error rate controlling procedures for discrete data. preprint, November 2017.

Proofs of Theorems

Proof of Theorem 2.1:

\Rightarrow : Immediate.

\Leftarrow :

Let $\mathcal{P}_x = \bigcup_{\mathbf{k}_{\{1, \dots, D_x\}} \in \mathbb{N}_0^{D_x}} \mathcal{P}^1 \times \dots \times \mathcal{P}^{D_x}$. Therefore $\sigma(\mathcal{P}_x) = \mathcal{B}([0, 1]^{D_x})$.

For $A_x \in \mathcal{B}([0, 1]^{D_x})$ let $[\mathbf{X} \in A_x] = \{\omega : \mathbf{X}(\omega) \in A_x\}$, then $\sigma(\mathbf{X}) = \{[\mathbf{X} \in A_x], A_x \in \mathcal{B}([0, 1]^{D_x})\}$.

Let $\mathcal{Q}_x = \bigcup_{\mathbf{k}_{\{1, \dots, D_x\}} \in \{-1, 0, 1, 2, \dots\}^{D_x}} \mathcal{Q}^{k_1} \times \dots \times \mathcal{Q}^{k_{D_x}}$ so that $\mathcal{Q}^{-1} := \emptyset$ and $\forall k \geq 0, \mathcal{Q}^k = \mathcal{P}^k$.

Let $\mathcal{C}_{\mathbf{X}} = \{[\mathbf{X} \in B_x], B_x \in \mathcal{Q}_x\}$.

Hence $\sigma(\mathcal{C}_{\mathbf{X}}) = \sigma(\mathbf{X}^{-1}(B_x), B_x \in \mathcal{Q}_x) = \sigma(\mathbf{X}^{-1}(\mathcal{Q}_x)) = \mathbf{X}^{-1}(\sigma(\mathcal{Q}_x)) = \mathbf{X}^{-1}(\sigma(\mathcal{P}_x)) = \sigma(\mathbf{X})$.

Note that $\mathcal{C}_{\mathbf{X}}$ is a π -system:

$E, E' \in \mathcal{C}_{\mathbf{X}} \Rightarrow E = \left[\mathbf{X} \in \left(\emptyset \text{ or } \left[\frac{l_1-1}{2^{k_1}}, \frac{l_1}{2^{k_1}} \right) \right) \times \dots \times \left(\emptyset \text{ or } \left[\frac{l_{D_x}-1}{2^{k_{D_x}}}, \frac{l_{D_x}}{2^{k_{D_x}}} \right) \right) \right]$ and
 $E' = \left[\mathbf{X} \in \left(\emptyset \text{ or } \left[\frac{l'_1-1}{2^{k'_1}}, \frac{l'_1}{2^{k'_1}} \right) \right) \times \dots \times \left(\emptyset \text{ or } \left[\frac{l'_{D_x}-1}{2^{k'_{D_x}}}, \frac{l'_{D_x}}{2^{k'_{D_x}}} \right) \right) \right]$ for some $\mathbf{l}, \mathbf{l}', \mathbf{k}, \mathbf{k}'$. Therefore:

$$\begin{aligned} E \cap E' &= \left[\mathbf{X} \in \left\{ \left(\emptyset \text{ or } \left[\frac{l_1-1}{2^{k_1}}, \frac{l_1}{2^{k_1}} \right) \right) \times \dots \times \left(\emptyset \text{ or } \left[\frac{l_{D_x}-1}{2^{k_{D_x}}}, \frac{l_{D_x}}{2^{k_{D_x}}} \right) \right) \right\} \cap \right. \\ &\quad \left. \left\{ \left(\emptyset \text{ or } \left[\frac{l'_1-1}{2^{k'_1}}, \frac{l'_1}{2^{k'_1}} \right) \right) \times \dots \times \left(\emptyset \text{ or } \left[\frac{l'_{D_x}-1}{2^{k'_{D_x}}}, \frac{l'_{D_x}}{2^{k'_{D_x}}} \right) \right) \right\} \right] \\ &= \left[\mathbf{X} \in \left(\emptyset \text{ or } \left[\frac{l_1-1}{2^{k_1}}, \frac{l_1}{2^{k_1}} \right) \cap \left[\frac{l'_1-1}{2^{k'_1}}, \frac{l'_1}{2^{k'_1}} \right) \right) \times \dots \right. \\ &\quad \left. \times \left(\left[\frac{l_{D_x}-1}{2^{k_{D_x}}}, \frac{l_{D_x}}{2^{k_{D_x}}} \right) \cap \left[\frac{l'_{D_x}-1}{2^{k'_{D_x}}}, \frac{l'_{D_x}}{2^{k'_{D_x}}} \right) \right) \right] \in \mathcal{C}_{\mathbf{X}} \end{aligned}$$

Similarly, define $\sigma(\mathbf{Y})$ and $\mathcal{C}_{\mathbf{Y}}$, another π -system, independent of $\mathcal{C}_{\mathbf{X}}$ and $\sigma(\mathbf{Y}) = \sigma(\mathcal{C}_{\mathbf{Y}})$.

By the basic criterion, then, $\sigma(\mathbf{X}) \perp \sigma(\mathbf{Y})$.

For the rest of this section we adopt the following notations:

Denote $X_1 = Z_1, \dots, X_{D_x} = Z_{D_x}$ and $Y_1 = Z_{D_x+1}, \dots, Y_{D_y} = Z_{D_y}$.

$\mathbf{d} \subset \{1, \dots, D\}$, $\mathbf{i} = \mathbf{d} \cap \{1, \dots, D_x\}$ and $\mathbf{j} = \{j : j + D_x \in \mathbf{d} \cap \{D_x + 1, \dots, D\}\}$

Denote

$$\begin{aligned}\mathbf{X}_{\mathbf{i}} &= \{X_i : i \in \mathbf{i}\}, & \mathbf{X}_{(\mathbf{i})} &= \{X_{i'} : i' \in \{1, \dots, D_x\} \setminus \mathbf{i}\} \\ \mathbf{Y}_{\mathbf{j}} &= \{Y_j : j \in \mathbf{j}\}, & \mathbf{Y}_{(\mathbf{j})} &= \{Y_{j'} : j' \in \{1, \dots, D_y\} \setminus \mathbf{j}\} \\ \mathbf{Z}_{\mathbf{d}} &= \mathbf{X}_{\mathbf{i}} \times \mathbf{Y}_{\mathbf{j}} = \{Z_d : d \in \mathbf{d}\}, & \mathbf{Z}_{(\mathbf{d})} &= \mathbf{X}_{(\mathbf{i})} \times \mathbf{Y}_{(\mathbf{j})} = \{Z_{d'} : d' \in \{1, \dots, D\} \setminus \mathbf{d}\}\end{aligned}$$

$$\begin{aligned}A_{x,\mathbf{d}} &= \bigotimes_{d \in \mathbf{d} \cap \{1, \dots, D_x\}} A_d, & A_{x,(\mathbf{d})} &= \bigotimes_{d' \in \{1, \dots, D_x\} \setminus \mathbf{d}} A_{d'} \\ A_{y,\mathbf{d}} &= \bigotimes_{d \in \mathbf{d} \cap \{D_x+1, \dots, D\}} A_d, & A_{y,(\mathbf{d})} &= \bigotimes_{d' \in \{D_x+1, \dots, D\} \setminus \mathbf{d}} A_{d'} \\ A_{\mathbf{d}} &= A_{x,\mathbf{d}} \times A_{y,\mathbf{d}} = \bigotimes_{d \in \mathbf{d}} A_d, & A_{(\mathbf{d})} &= A_{x,(\mathbf{d})} \times A_{y,(\mathbf{d})} = \bigotimes_{d' \in \{1, \dots, D\} \setminus \mathbf{d}} A_{d'}\end{aligned}$$

$$\mathbf{k}_{\mathbf{d}} = \{k_d : d \in \mathbf{d}\}, \quad \mathbf{k}_{(\mathbf{d})} = \{k_{d'} : d' \in \{1, \dots, D\} \setminus \mathbf{d}\}$$

Definition 6.1. *Conditional \mathbf{k} -independence:*

We say that $\mathbf{X}_{\mathbf{i}}$ and $\mathbf{Y}_{\mathbf{j}}$ are \mathbf{k} -independent conditional on $\mathbf{Z}_{(\mathbf{d})}$ and write it as $\mathbf{X}_{\mathbf{i}} \perp_{\mathbf{k}} \mathbf{Y}_{\mathbf{j}} \mid \mathbf{Z}_{(\mathbf{d})}$ if for any $A \in \mathcal{A}^{\mathbf{k}}$:

$$\mathbb{P}(\mathbf{X}_{\mathbf{i}} \in A_{x,\mathbf{d}}, \mathbf{Y}_{\mathbf{j}} \in A_{y,\mathbf{d}} \mid \mathbf{Z}_{(\mathbf{d})} \in A_{(\mathbf{d})}) = \mathbb{P}(\mathbf{X}_{\mathbf{i}} \in A_{x,\mathbf{d}} \mid \mathbf{Z}_{(\mathbf{d})} \in A_{(\mathbf{d})}) \cdot \mathbb{P}(\mathbf{Y}_{\mathbf{j}} \in A_{y,\mathbf{d}} \mid \mathbf{Z}_{(\mathbf{d})} \in A_{(\mathbf{d})})$$

Or equivalently:

$$\mathbb{P}(\mathbf{X}_{\mathbf{i}} \in A_{x,\mathbf{d}} \mid \mathbf{Y}_{\mathbf{j}} \in A_{y,\mathbf{d}}, \mathbf{Z}_{(\mathbf{d})} \in A_{(\mathbf{d})}) = \mathbb{P}(\mathbf{X}_{\mathbf{i}} \in A_{x,\mathbf{d}} \mid \mathbf{Z}_{(\mathbf{d})} \in A_{(\mathbf{d})})$$

When $k_{d'} = 0$ for some $d' \in \{1, \dots, D\} \setminus \mathbf{d}$, $\Omega_{Z_{d'}} = [0, 1]$ for those indices and hence our notation may be compacted. For example, if $k_{d'} = 0$ for all $d' \in \{1, \dots, D\} \setminus \mathbf{d}$:

$$\mathbf{X}_{\mathbf{i}} \perp_{\mathbf{k}} \mathbf{Y}_{\mathbf{j}} \mid \mathbf{Z}_{(\mathbf{d})} \Leftrightarrow \mathbf{X}_{\mathbf{i}} \perp_{\mathbf{k}_{\mathbf{d}}} \mathbf{Y}_{\mathbf{j}}$$

Definition 6.2. For $A_d \in \mathcal{P}^{k_d-1}$ such that $A_d = [\frac{l_d-1}{2^{k_d-1}}, \frac{l_d}{2^{k_d-1}})$, define $A_d^0 = [\frac{2l_d-2}{2^{k_d}}, \frac{2l_d-1}{2^{k_d+1}}) \in \mathcal{P}^{k_d}$ and

$A_d^1 = [\frac{2l_d-1}{2^{k_d+1}}, \frac{2l_d}{2^{k_d+1}}) \in \mathcal{P}^{k_d}$. Note that $A_d = A_d^0 \sqcup A_d^1$.

Proof of Lemma 2.1:

Let $F_{\mathbf{X}}$ be the probability distribution of \mathbf{X} and $F_{\mathbf{Y}}$ be the probability distribution of \mathbf{Y} .

Then $\mathbf{X} \perp_{\mathbf{k}} \mathbf{Y} \Leftrightarrow F(A) = F_{\mathbf{X}}(A_x)F_{\mathbf{Y}}(A_y)$ for all $A \in \mathcal{A}^{\mathbf{k}}$.

It is enough to show that $\mathbf{X} \perp_{\mathbf{k}} \mathbf{Y} \Rightarrow \mathbf{X} \perp_{\mathbf{k}'} \mathbf{Y}$ for any \mathbf{k}' such that (i) $k'_i = k_i - 1$ for some $i \in \{1, \dots, D_x\}$ and (ii) $k'_d = k_d$ for all $d \in \{1, \dots, D\} \setminus \{i\}$.

Hence, assuming $\mathbf{X} \perp_{\mathbf{k}} \mathbf{Y}$ we get for $A \in \mathcal{A}^{\mathbf{k}'}$ that:

$$\begin{aligned} F(A) &= F(A_1 \times \dots \times A_{i-1} \times A_i^0 \times A_{i+1} \times \dots \times A_{D_x} \times A_y) \\ &\quad + F(A_1 \times \dots \times A_{i-1} \times A_i^1 \times A_{i+1} \times \dots \times A_{D_x} \times A_y) \\ &= F_{\mathbf{X}}(A_1 \times \dots \times A_{i-1} \times A_i^0 \times A_{i+1} \times \dots \times A_{D_x}) F_{\mathbf{Y}}(A_y) \\ &\quad + F_{\mathbf{X}}(A_1 \times \dots \times A_{i-1} \times A_i^1 \times A_{i+1} \times \dots \times A_{D_x}) F_{\mathbf{Y}}(A_y) \\ &= F_{\mathbf{X}}(A_x) F_{\mathbf{Y}}(A_y) \end{aligned}$$

As required.

We next provide a discretized version of some basic results in probability:

Lemma 6.1. *Contraction:*

For $\mathbf{d} \subset \{1, \dots, D\}$ such that $\{1, \dots, D_x\} \subset \mathbf{d}$ (i.e. $\mathbf{i} = \{1, \dots, D_x\}$, $\mathbf{X}_{\mathbf{i}} = \mathbf{X}$ and $\mathbf{Y}_{(\mathbf{j})} = \mathbf{Z}_{(\mathbf{d})}$):

$$\begin{cases} \mathbf{X} \perp_{\mathbf{k}} \mathbf{Y}_{\mathbf{j}} \mid \mathbf{Z}_{(\mathbf{d})} \\ \mathbf{X} \perp_{\mathbf{k}_{(\mathbf{d})}} \mathbf{Y}_{(\mathbf{j})} \end{cases} \Rightarrow \mathbf{X} \perp_{\mathbf{k}} \mathbf{Y}$$

Proof: Immediate from definition.

Lemma 6.2. *Decomposition:*

For $\mathbf{d} \subset \{1, \dots, D\}$ such that $\{1, \dots, D_x\} \subset \mathbf{d}$ (i.e. $\mathbf{i} = \{1, \dots, D_x\}$ and $\mathbf{X}_{\mathbf{i}} = \mathbf{X}$):

$$\mathbf{X} \perp_{\mathbf{k}} \mathbf{Y} \Rightarrow \begin{cases} \mathbf{X} \perp_{\mathbf{k}_{\mathbf{d}}} \mathbf{Y}_{\mathbf{j}} \\ \mathbf{X} \perp_{\mathbf{k}_{(\mathbf{d})}} \mathbf{Y}_{(\mathbf{j})} \end{cases}$$

Proof: Immediate from definition.

Lemma 6.3. *Weak Union:*

For $\mathbf{d} \subset \{1, \dots, D\}$ such that $\{1, \dots, D_x\} \subset \mathbf{d}$ (i.e. $\mathbf{i} = \{1, \dots, D_x\}$, $\mathbf{X}_{\mathbf{i}} = \mathbf{X}$, $\mathbf{Y}_{\mathbf{j}} = \mathbf{Z}_{\mathbf{d}}$ and $\mathbf{Y}_{(\mathbf{j})} = \mathbf{Z}_{(\mathbf{d})}$):

$$\mathbf{X} \perp_{\mathbf{k}} \mathbf{Y} \Rightarrow \begin{cases} \mathbf{X} \perp_{\mathbf{k}} \mathbf{Y}_{\mathbf{j}} \mid \mathbf{Z}_{(\mathbf{d})} \\ \mathbf{X} \perp_{\mathbf{k}} \mathbf{Y}_{(\mathbf{j})} \mid \mathbf{Z}_{\mathbf{d}} \end{cases}$$

Proof: Immediate from definition.

Definition 6.3. Given $\mathbf{k} \in \mathbb{N}_0^D$ and $i \in \{1, \dots, D_x\}$, $j \in \{1, \dots, D_y\}$ let

$$\begin{aligned} [k_i, k_j](\mathbf{k}_{<i, <j}) &= \{\mathbf{k}' \in \mathbb{N}_0^D : && k'_i < k_i, k'_j < k_j \text{ and} \\ &&& k'_d = k_d \text{ for all } d \in \{1, \dots, i-1\} \cup \{D_x+1, \dots, D_x+j-1\} \\ &&& \text{and} \\ &&& k'_d = 0 \text{ for all } d \in \{i+1, \dots, D_x\} \cup \{D_x+j+1, \dots, D\}\} \end{aligned}$$

Accordingly,

$$\mathcal{A}^{[k_i, k_j](\mathbf{k}_{<i, <j})} = \bigcup_{\mathbf{k}' \in [k_i, k_j](\mathbf{k}_{<i, <j})} \mathcal{A}^{\mathbf{k}'}$$

denote the totality of all cuboids in strata that are coarser than the stratum $\mathcal{A}^{\mathbf{k}}$ along the margins i and j such that margins $\{i+1, \dots, D_x\}$ and $\{D_x+j+1, \dots, D\}$ are allowed any value in $[0, 1]$.

Proof of Theorem 2.2:

\Rightarrow :

Assume $\mathbf{X} \perp_{\mathbf{k}} \mathbf{Y}$ for some $\mathbf{k} \in \mathbb{N}_0^D$.

Let $i \in \{1, \dots, D_x\}$ and $j \in \{1, \dots, D_y\}$.

By applying the weak union lemma twice we get that $X_i \perp_{(k_i, k_{D_x+j})} Y_j \mid \mathbf{Z}_{(\{i, D_x+j\})}$.

Notice that for \mathbf{k}' such that $k'_i = k_i - 1$, $k'_{D_x+j} = k_{D_x+j} - 1$, $k'_d = k_d$ for all $d \in \{1, \dots, D\} \setminus \{i, D_x+j\}$ and $A \in \mathcal{A}^{\mathbf{k}'}$ we get that $A_{ij}^{00}, A_{ij}^{11}, A_{ij}^{01}, A_{ij}^{10} \in \mathcal{A}^{\mathbf{k}}$. So $\theta_{ij}(A) = 0$ by the definition of conditional independence and the LOR.

By Lemma 2.1 we get that indeed $\theta_{ij}(A) = 0$ for $A \in \mathcal{A}^{[k_i, k_j]}$.

\Leftarrow :

First, notice that it suffices to show that:

$$\begin{aligned} \mathbf{X} \perp_{\mathbf{k}} \mathbf{Y} \iff \theta_{ij}(A) = 0 \\ \forall i \in \{1, 2, \dots, D_x\}, \quad j \in \{D_x+1, \dots, D\}, \quad A \in \mathcal{A}^{[k_i, k_j](\mathbf{k}_{<i, <j})} \end{aligned}$$

Since then we may rely on the opposite direction to get that $\theta_{ij}(A) = 0$ for all $A \in \mathcal{A}^{[k_i, k_j]}$.

Examine

$$X_i \perp\!\!\!\perp_{\mathbf{k}_{\{1, \dots, i, D_x+1, \dots, D_x+j\}}} Y_j \mid \mathbf{X}_{\{1, \dots, i-1\}}, \mathbf{Y}_{\{1, \dots, j-1\}}$$

To see that the above is true, let $\mathbf{k}' \in \mathbb{N}_0^D$ such that $k'_d = k_d$ for all $d \in \{1, \dots, i\} \cup \{D_x + 1, \dots, D_x + j\}$ and $k'_d = 0$ for all $d \in \{i + 1, \dots, D_x\} \cup \{D_x + j + 1, \dots, D\}$.

For a given $A \in \mathcal{A}^{\mathbf{k}'}$ let x, y be a pair of univariate random variables whose joint distribution is given by $G := F_{X_i, Y_j \mid \mathbf{X}_{\{1, \dots, i-1\}} \in A_x, \{1, \dots, i-1\}, \mathbf{Y}_{\{1, \dots, j-1\}} \in A_y, \{D_x+1, \dots, D_x+j-1\}}$. By assumption:

$$\begin{aligned} 0 = \theta_{ij}(A) &= \log \frac{F(A_{ij}^{00}) \cdot F(A_{ij}^{11})}{F(A_{ij}^{01}) \cdot F(A_{ij}^{10})} \\ &= \log \frac{G(A_i^0 \times A_{D_x+j}^0) \cdot G(A_i^1 \times A_{D_x+j}^1)}{G(A_i^0 \times A_{D_x+j}^1) \cdot G(A_i^1 \times A_{D_x+j}^0)} \end{aligned}$$

Since the above holds for every $A \in \mathcal{A}^{[k_i, k_j] (\mathbf{k}_{<i, <j})}$ we may apply Theorem 2 from Ma and Mao [7] and conclude that $x \perp\!\!\!\perp_{(k_i, k_{D_x+j})} y$ which is equivalent to $X_i \perp\!\!\!\perp_{\mathbf{k}_{\{1, \dots, i, D_x+1, \dots, D_x+j\}}} Y_j \mid \mathbf{X}_{\{1, \dots, i-1\}}, \mathbf{Y}_{\{1, \dots, j-1\}}$.

Next, examine:

$$\begin{aligned}
(\star) & \left\{ \begin{array}{l} X_1 \perp\!\!\!\perp_{\mathbf{k}_{\{1, D_x+1\}}} Y_1 \\ X_1 \perp\!\!\!\perp_{\mathbf{k}_{\{1, D_x+1, D_x+2\}}} Y_2 \mid Y_1 \\ X_1 \perp\!\!\!\perp_{\mathbf{k}_{\{1, D_x+1, D_x+2, D_x+3\}}} Y_3 \mid \mathbf{Y}_{\{1,2\}} \\ \vdots \\ X_1 \perp\!\!\!\perp_{\mathbf{k}_{\{1, D_x+1, \dots, D-1\}}} Y_{D_y-1} \mid \mathbf{Y}_{\{1, \dots, D_y-2\}} \\ X_1 \perp\!\!\!\perp_{\mathbf{k}_{\{1, D_x+1, \dots, D\}}} Y_{D_y} \mid \mathbf{Y}_{\{1, \dots, D_y-1\}} \end{array} \right. \\
(\star\star) & \left\{ \begin{array}{l} X_2 \perp\!\!\!\perp_{\mathbf{k}_{\{1,2, D_x+1\}}} Y_1 \mid X_1 \\ X_2 \perp\!\!\!\perp_{\mathbf{k}_{\{1,2, D_x+1, D_x+2\}}} Y_2 \mid X_1, Y_1 \\ \vdots \\ X_2 \perp\!\!\!\perp_{\mathbf{k}_{\{1,2, D_x+1, \dots, D\}}} Y_{d_y} \mid X_1, \mathbf{Y}_{\{1, \dots, D_y-1\}} \\ \vdots \end{array} \right. \\
(\star\star\star) & \left\{ \begin{array}{l} X_{D_x} \perp\!\!\!\perp_{\mathbf{k}_{\{1, \dots, D_x, D_x+1\}}} Y_1 \mid \mathbf{X}_{\{1, \dots, D_x-1\}} \\ X_{D_x} \perp\!\!\!\perp_{\mathbf{k}_{\{1, \dots, D_x, D_x+1, D_x+2\}}} Y_2 \mid \mathbf{X}_{\{1, \dots, D_x-1\}}, Y_1 \\ \vdots \\ X_{D_x} \perp\!\!\!\perp_{\mathbf{k}} Y_{D_y} \mid \mathbf{X}_{\{1, \dots, D_x-1\}}, \mathbf{Y}_{\{1, \dots, D_y-1\}} \end{array} \right.
\end{aligned}$$

Each of the above rows is obtained by the previous argument. Applying the contraction lemma recursively from top to bottom to each of the rows in (\star) shows that $X_1 \perp\!\!\!\perp_{\{1, D_x, \dots, D\}} \mathbf{Y}$. Further applying the contraction lemma to the latter result and the rows of $(\star\star)$ shows that $\mathbf{X}_{\{1,2\}} \perp\!\!\!\perp_{\{1,2, D_x, \dots, D\}} \mathbf{Y}$. And a similar application of the contraction lemma to the previous results and all the rows up to $(\star\star\star)$ shows that $\mathbf{X} \perp\!\!\!\perp_{\mathbf{k}} \mathbf{Y}$. \square

Note, for every $i \in \{1, \dots, D_x\}$ and $j \in \{1, \dots, D_y\}$, and for each of the above conditions $X_i \perp\!\!\!\perp_{\mathbf{k}_{\{1, \dots, i-1, D_x+1, \dots, D_x+j\}}} Y_j \mid \mathbf{X}_{\{1, \dots, i-1\}}, \mathbf{Y}_{\{1, \dots, j-1\}}$ there are $(2^{k_i} - 1)(2^{k_j} - 1)$ one degrees of freedom tests required, each repeated due to the conditioning $\prod_{s=1}^{i-1} 2^{k_s} \cdot \prod_{t=D_x+1}^{D-1} 2^{k_t}$ times. Summing over j , we get that for each i , there are $(2^{k_i} - 1) \cdot \prod_{s=1}^{i-1} 2^{k_s} \cdot (2^{\sum_{t=D_x+1}^D k_t} - 1)$ one degrees of freedom tests. Summing those over i we get that overall we need to perform $(2^{\sum_{s=1}^{D_x} k_s} - 1)(2^{\sum_{t=D_x+1}^D k_t} - 1)$ one degrees of freedom tests.

Under H_1 there are $2^{\sum_{s=1}^{D_x} k_s} \cdot 2^{\sum_{t=D_x+1}^D k_t} - 1$ degrees of freedom, under H_0 there are $(2^{\sum_{s=1}^{D_x} k_s} - 1) + (2^{\sum_{t=D_x+1}^D k_t} - 1)$ degrees of freedom, and thus we need $(2^{\sum_{s=1}^{D_x} k_s} - 1)(2^{\sum_{t=D_x+1}^D k_t} - 1)$ degrees of freedom to identify a difference between the null and the alternative. It follows from the proof that we may indeed use $(2^{\sum_{s=1}^{D_x} k_s} - 1)(2^{\sum_{t=D_x+1}^D k_t} - 1)$ 1-degree of freedom independence tests to do so.